Supporting Information for

Microenvironment-responsive release of Mg^{2+} from tannic acid decorated and multilevel crosslinked hydrogel accelerates infected wound healing

Na Li[1,2,3], Yi Cao[1,2], Jingyi Liu[1,2], Wen Zou[1,2,3], Manyu Chen[1,2], Hongfu Cao[1,2], Siyan Deng[1,2], Jie Liang[1,2,3], Tun Yuan[1,2,3], Yujiang Fan[1, 2], Qiguang Wang[1,2*], Xingdong Zhang[1,2]*

[1] National Engineering Research Center for Biomaterials, Sichuan University, 29# Wangjiang Road, Chengdu, Sichuan, 610064, China.

[2] College of Biomedical Engineering, Sichuan University, 29# Wangjiang Road, Chengdu, Sichuan 610064, China.

[3] Sichuan Testing Center for Biomaterials and Medical Devices, Sichuan University, 29# Wangjiang Road, Chengdu 610064, China.

Corresponding authors:

* Yujiang Fan email: fan_yujiang@scu.edu.cn

* Qiguang Wang email: wqgwang@126.com

Material and Methods

Physicochemical Analysis

The molecular composition of OHA and OHA-P was examined by Nuclear Magnetic Resonance (^{1}H NMR, 400 MHz, Bruker AMX-400, USA). The structural integrity of the hydrogel was assessed by Attenuated Total Reflection Fourier Transform Infrared Spectroscopy (ATR-FTIR, Nicolet 6700, Thermo Electron Corporation, USA) within the range of 4000-500 cm^{-1}. The microstructure of the OHA-P-TA/G hydrogels was visualized using Scanning Electron Microscopy (SEM, HITACHI S-800, Japan). Images were analyzed by using Image J software.

The prepared hydrogels were subjected to dynamic mechanical analyzer (DMA) (TA, Q800, USA) for force testing. The storage modulus (G') and loss modulus of the three hydrogels were tested at 1 Hz, 2 Hz, 5 Hz, 10 Hz, 40 Hz, 60 Hz, 80 Hz and 100 Hz, respectively, the energy storage modulus (G') and loss modulus (G″) of the hydrogels were tested at room temperature. The specific test parameters include: pre-compressive stress of 0.005 N, amplitude of 40 μm, dynamic-static force ratio of 105%.

The rheological properties of the disk-shaped hydrogels (25 mm × 1 mm) were evaluated at ambient temperature using a rheometer (TA, HR20, USA). The storage modulus (G′) and the loss modulus (G″) varied over time when UV irradiation commenced after a duration of 30 s and was documented for 100 s. With constant strain amplitude of $\gamma = 0.5\%$，The storage modulus (G′) and the loss modulus (G″) varied over frequency range between 0.1 and 10 Hz. The viscosity changes of the four hydrogels were tested at 37 ℃. The specific parameters of the test included: the time of taking points was from the steady state, the shear rate from 0.1 to 10 (1/s). The modulus varied over oscillating shear stress change (1%-760%).

The mechanism of interaction of OHA-P-TA/G/Mg^{2+} was studied by X-ray photoelectron spectroscopy (XPS) (Kratos AXIS ULTRA DLD). C_{1s} binding energy (284.6eV) was selected as the standard for energy correction.

The phase composition of the samples was scrutinized using X-ray diffraction (XRD, X'Pert Pro MPD DY129, PANalytical), employing a step duration of 1 s within the 2θ range of 20° to 80°.

The thermostability of the modified OHA-P-TA/G/Mg^{2+} hydrogel was assessed using a thermal gravimetric analyzer (TG 209 F3, Netzsch), with a heating rate of 10 °C/min from room temperature to 400 °C in an air flow.

Differential scanning calorimetry (DSC) was adopted to test crystallinities of OHA-P-TA/G/Mg^{2+} hydrogel from 50 °C to 400 °C at a rate of 20 °C/min under an Argon atmosphere with a flow rate of 50 ml/min.

The EDS mapping for the Mg elements of the OHA-P-TA/G and OHA-P-TA/G/Mg^{2+} was carried out using SEM. The porosity and pore size distribution curve were determined through the mercury intrusion technique (AutoPore 9500, Micromeritics).

Hydrogel Swelling Analysis

The equilibrated swelling ratios of the composites were calculated. In brief, the initial weight of disk-shaped hydrogels (10 mm × 1 mm) (W_0) was recorded and then completely submerged in 10 mL PBS solution (pH 7.4) and acidic (pH 4.5) at 37 ℃ with shaking at 100 rpm. The gel block was carefully pipetted with filter paper to remove the surface solution was weighed (W_t), at various time intervals (30, 60, 120, 240, 480, and 720 h) until the hydrogels reached swelling equilibrium. The swelling ratio SRs was calculated using the following equation:

$$\text{Swelling ratio (\%)} = (W_t - W_0) / W_0 \times 100\%$$

In vitro Degradation Analysis

The remaining weight ratio of the composites was calculated. In brief, the initial weight of disk-shaped hydrogels (10 mm × 1 mm) (W_0) was recorded and then completely submerged in 10 mL PBS solution (pH 7.4) and acidic (pH 4.5) at 37℃ with shaking at 100 rpm. The samples were completely dried and weighed (W_t) at various time intervals (0, 1, 2, 3, 4, 5, and 6 days). The *in vitro* remaining ratio was computed using the following formula:

$$\text{Remaining ratio (\%)} = (W_t / W_0) \times 100\%$$

Investigation of TA and Mg^{2+} Release Characteristics

Briefly, 0.1 g of the dried hydrogels were submerged in 5 mL of various solutions and placed into a shaker incubator at 100 rpm at 37 °C. At pre-determined time points, 1 mL of the hydrogels' release media was removed and substituted with 1 mL of fresh PBS solution to keep the overall volume of the release medium steady (5 mL). The cumulative concentration of TA released from the hydrogels was measured in accordance with the calibration curve and UV-vis spectroscopy at 278 nm.

The OHA-TA/G/Mg^{2+} hydrogel was submerged in 5 mL of various solutions (pH 7.4, 4.5, 9.0), and the solution was subjected to shaking at 120 rpm at a temperature of 37 °C for a duration of 2 days. At specific time intervals, 1 mL of the solution was extracted to gauge the quantity of Mg^{2+} released, and an equal volume of fresh PBS was supplemented.

Intracellular Reactive Oxygen Species (ROS) Level

The intracellular ROS level was assessed using a fluorometric intracellular ROS Kit (Beyotime Biotechnology, S0033). To summarize, 1×10^4 L929 cells were seeded in 24-well plates and a cellular oxidative damage model was established using 100 μM H_2O_2. Following this, the cells underwent treatment with each hydrogel extracts for a period of 24 h. For the negative control (NC) group, the cells were solely treated with a complete medium. For the positive control (PC) group, the cells were treated with a complete medium contained 100 μM H_2O_2, loading DCFH-DA probe. Afterward, the fluorescence signal image was captured using a fluorescence microscope post a 20 min

incubation with the DCFH-DA probe. The expression of ROS mean fluorescence intensity was quantified using Image J software.

ABTS Radical Scavenging

The stock solutions comprised a 7.4 mM ABTS+ solution and a 2.6 mM potassium persulfate solution. The operational solution was subsequently formulated by combining equal amounts of the two base solutions and permitting them to interact for a duration of 12 h at ambient temperature in a dark environment. The solution was then diluted using PBS to achieve an absorbance of 0.7 ± 0.02 units at 734 nm, as measured by the microplate reader. A fresh ABTS+ solution was formulated for each test. The hydrogels were subjected to a reaction with 100 μL of the ABTS+ working solution for a duration of 30 min in a dark environment. The absorbance was measured at 734 nm utilizing the microplate reader (Spectra MaxM2, Molecular Devices, Sunnyvale, CA, USA).

The ABTS Radical Scavenging (%) was calculated as = $(A - A_0) / A \times 100\%$

where A represented the absorption of the blank (solely the ABTS+ ethanol solution) and A_0 denoted the absorption of the sample.

DPPH Radical Scavenging Activity

The DPPH radical scavenging activity of the hydrogels was assessed following a method outlined in an earlier research.[1] Each hydrogel was combined with 0.2 mL of a 0.4 mM DPPH ethanol solution for a duration of 10 min. Subsequently, the wavelength of DPPH was scanned using a UV-vis spectrophotometer at 517 nm. The DPPH scavenging was computed using the subsequent formula:

$$\text{DPPH scavenging (\%)} = (A_0 - A_1) / A_0 \times 100\%$$

Where A_0 represents the absorption of the blank (solely the DPPH ethanol solution) and A1 denotes the absorption of the sample.

Antibacterial Properties

The antibacterial properties of each hydrogel were assessed using Escherichia coli (*E. coli*, ATCC 25922) and Staphylococcus aureus (*S. aureus*, ATCC 25923). In

brief, a single bacterial colony was grown in 10 mL of Tryptic Soy Broth (TSB) and incubated at a temperature of 37 °C for a duration of 12 h. Following this, 1×10^4 CFUs in 1 mL of bacterial suspensions were evenly combined with each sterilized hydrogel and cultivated statically. After a period of 12 h, the mixed culture solution was diluted by a factor of 10^5 and uniformly spread onto Tryptone Soy Agar (TSA), followed by an incubation period of 24 h. Subsequently, the count of individual colonies in each group was documented. The bacterial survival rate was c calculated using the following formula:

$$\text{Antibacterial rate (\%)} = N_0 / N_1 \times 100\%$$

where N_1 represents the bacterial count for each hydrogel and N_0 represents the bacterial count for the control group with only bacterial suspension.

The agar diffusion assay was employed to measure the antibacterial ability in the surface diffusion of the hydrogel by analyzing the zone of inhibition (ZOI). Briefly, 200 μL suspension of bacteria at 1×10^6 CFUs/mL concentration was evenly plated onto TSA. After that, each sterile hydrogel of the same size was attached to the center of the TSA, cultured statically at 37 °C, and photographed at a specific time to quantify the size of antibacterial belt's outer diameter.

Cytotoxicity and Cell Proliferation

L929 cells were employed to examine the direct and indirect cytocompatibility of the hydrogels. The cells were cultivated in Dulbecco's Modified Eagle Medium (DMEM) that contained 10% fetal bovine serum and were placed in an incubator at a temperature of 37 ℃ with 5% CO_2. The hydrogel extract was prepared by submerging sterile disk-shaped hydrogels (10 mm × 1 mm) in 1 mL of serum-free medium for 24 h. We co-cultured each group of hydrogel extracts with L929 cells for 1, 3, and 5 days, respectively, and then performed FDA/PI staining and Cell Counting Kit-8 (CCK-8, Beyotime, Shanghai, China) assay to measure the optical density (OD) of the solution at 450 nm.

Cell Migration

The migration of cells was assessed using a cell scratch assay treatment with each hydrogel extracts with 100 μM H_2O_2 induced L929 cells. Firstly, 1×10^5 of L929 cells were grown in the complete medium until they achieved 80% confluence, at which point a scratch was created using a sterile 200 μL pipette tip. Following this, the sterile hydrogel extracts and cells were co-cultured in a state of serum deprivation, with the control group being treated solely with serum-free medium. The scratch of cells was imaged using an inverted microscope at 0 and 24 h respectively. The rate of migration was computed using the subsequent formula:

$$\text{Migration rate (\%)} = (A_0 - A_1) / A0 \times 100\%$$

where A_1 represents the scratch width after sample treatment and A_0 represents the initial scratch width.

Tube Formation Assay

The ability to form tubes was assessed using Matrigel Matrix (Corning, 356231, US) following a previously described method.[2] A volume of 50 μL of Matrigel was introduced into pre-cooled 96-well plates and then incubated at a temperature of 37 ℃ in a 5% CO_2 environment for a duration of 1 h. HUVECs (2×10^4 cells), which had undergone pre-treatment with different hydrogel extracts for a period of 48 h, along with HUVECs that were not subjected to any treatment, were then planted in the plates. Following a period of 10 h, the formation of tubules was visually inspected using an optical microscope, and the count of meshes per field was quantified using Image J software.

Hemolysis assay

The hemolysis assay was conducted as outlined in a prior study, albeit with a few modifications. In brief, selected healthy extracted fresh rabbit blood, every 10 mL fresh rabbit blood add 2% potassium oxalate solution 0.5 mL, gently mixed, made of fresh anticoagulated rabbit blood, placed in 4 ℃ conditions, within 48 h use. Add about 10mL of 0.9% sodium chloride injection to every 8 mL of fresh anticoagulated rabbit

blood to make diluted anticoagulated rabbit blood. Centrifuge the arterial blood in the anticoagulated tube at 1500 rpm for 15 min, remove the upper layer of plasma and retain the lower layer of blood cell precipitate, and then resuspend it twice by adding 0.9% NaCl to achieve a 4% (v/v) solution. The hydrogel was introduced into the 0.9% NaCl solution, which was then combined with the 4% (v/v) solution in equal volumes and incubated at 37 °C for 1 h. Following this, the supernatant (A) was subjected to centrifugation and its absorbance was gauged at 450 nm. PBS (A_n) and 0.1% Triton-X100 (A_p) were incorporated as the negative and positive controls, respectively. The hemolysis rate was computed using the formula: Hemolysis rate (%) = $(A - A_n) / (A_p - A_n) \times 100\%$

Anti-Inflammatory Capability

RAW 264.7 macrophages were incubated for 12 h in DMEM containing lipopolysaccharide (LPS, 1 μg/mL), after which they were incubated with various hydrogel extracts. The intracellular level of NO was detected by DAF-FM DA (Beyotime S0019S) and Nitric oxide NO content test kit (Shanghai Enzyme-linked Biotechnology, 287810).

Regulation of Macrophage Phenotype

RAW 264.7 macrophages (1×10^6 cells) that had undergone pre-treatment with LPS for a duration of 12 h were subjected to incubation with a variety of extracts of hydrogel in 6-well plates. Following an incubation period of 24 h, the cells were collected through centrifugation and rinsed twice using cold PBS. The treated cells were then stained with FITC-tagged anti-CD86 antibodies and APC-tagged CD206 as per the instructions provided by the manufacturer, and subsequently analyzed using flow cytometry (BD Biosciences). The data was processed using FlowJo software (Tree Star).

Immunofluorescence Test

RAW264.7 cells were propagated in DMEM enriched with 10% FBS and 1% PS. RAW 264.7 macrophages (1×10^6 cells) that had undergone pre-treatment with LPS for a duration of 12 h were subjected to incubation with a variety of extracts of hydrogel in 6-well plates. After fixing the cells, the primary antibody (INOS and CD206+) was added and incubated for 0.5 h. Upon three times washing, the secondary antibody was added and incubated for 1 h, followed by DAPI staining and observation.

PCR Analysis

RAW 264.7 macrophages (2×10^5 cells) that had been pre-treated with LPS (1 μg/mL) for a duration of 12 h. Following a period of 24 h incubated with extracts from the hydrogel in 6-well plates, the cells were gathered, the RNA extraction was carried out using the RNeasy Mini kit (Qiagen) as per the guidelines provided by the manufacturer, after which it was transformed into cDNA using the iScript™ cDNA Synthesis Kit (Bio-Rad, USA). qPCR analysis was conducted using SYBR Green (Roche, USA) on a C1000™ Thermal cycler machine (Bio-Rad, USA). The relative levels of gene expression were computed using the $2^{-\Delta\Delta CT}$ formula. β-Actin mRNA was utilized for PCR amplification, and quantitative real-time PCR was used to ascertain the mRNA expression. The sequences of the primers (5′-3′) employed in this research are listed in in Table S1.

In vivo Wound Healing

The infected mice were randomly divided into four groups: control group (n=6), OHA-P/G group (n=6), OHA-P-TA/G group (n=6) and OHA-P-TA/G/Mg^{2+} group (n=6). After infecting 1 day, hydrogel precursor solutions were injected into the wound and then blue light (15 mW) for a duration for 60 s, the control group was treated commercial Tegaderm film. The wounds were then treated with iodophor disinfection with commercial Tegaderm film, the dressings were changed every three days. The progression of the wounds was documented through photograph taken at day 0, 3, 6, 8, and 12, and the wound areas were quantified using Image J software.

$$\text{Wound closure (\%)} = (A_0 - A_t) / A_0 \times 100\%$$

where A_t and A_0 were the wound areas on day t and day 0, respectively.

In vivo Antibacterial ability Test

On day 2, infected tissue samples were gathered and meticulously mixed with 2 mL of TSB in a sterile environment. This mixture was then diluted by a factor of 1000x. The resulting bacterial suspension was spread onto TSA plates and incubated at a temperature of 37 ℃ for a period of 12 h. This process allowed for the formation of visible colony units.

Immunohistochemistry and ELISA Test

To evaluate the epidermal regeneration of the epidermal layer in wound tissue, mice were humanely euthanized at a specified time point. The wound tissues were then harvested and immersed in a 4% (vol/vol) solution of paraformaldehyde for a duration of 24 h. Following this, the tissues were dehydrated using a series of alcohols and subsequently embedded in paraffin. Each paraffin block was sectioned into slices of 4 μm thickness and stained using hematoxylin and eosin (H&E), Masson's trichrome, and immunohistochemistry for analysis (TNF-α, IL-6, IL-4, Ki67 and VEGF). The statistics of collagen deposition, the number of blood vessels, TNF-α, IL-6, IL-4, Ki67 and VEGF were measured by Image J software. On the 6^{th} day, the mice were euthanized and the orbital blood was collected and centrifuged for ELISA. Cytokines were measured by commercial ELISA kits (Jiangsu MEIMIAN): TNF-α, IL-6, IL-4 and VEGF, following the manufacturer's guidance.

Histological Analysis

The process of epidermal regeneration in wound tissues was evaluated using various staining techniques such as hematoxylin and eosin (H&E), Masson's trichrome, Sirus red staining, and immunohistochemical staining. The mice were humanely euthanized on day 6 and 12, post which the wound tissues were immersed in a 4%

paraformaldehyde solution for a duration of 24 h. Following this, the tissues subsequently embedded in paraffin.

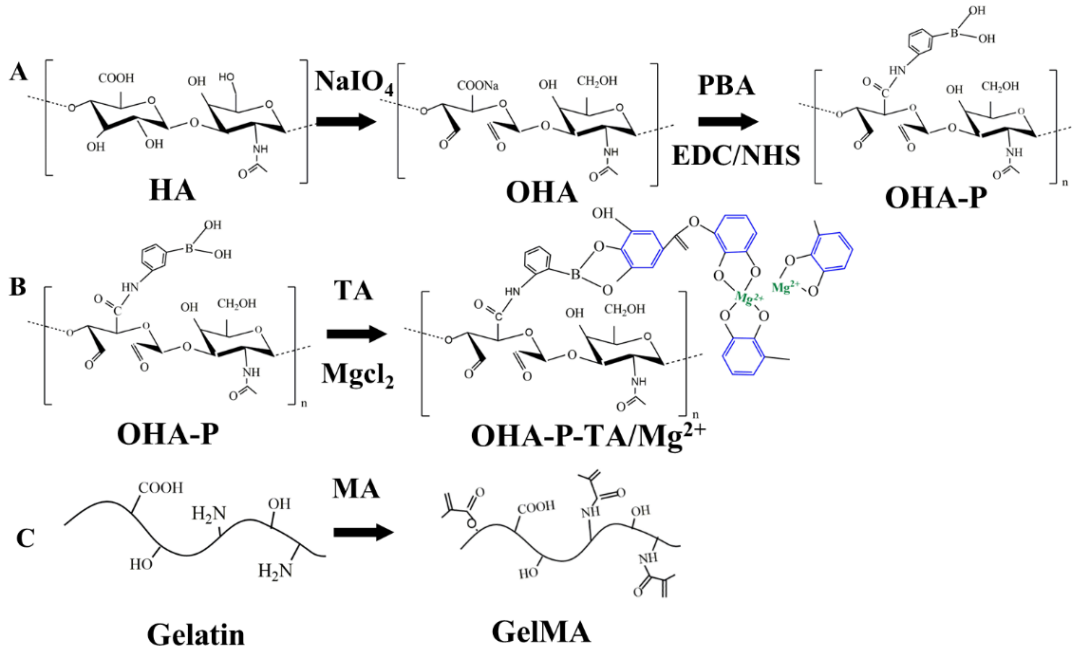

Fig. S1. Synthetic route of OHA-P-TA/G/Mg^{2+} hydrogel. A. Synthetic route of OHA-P. B. Synthetic route of OHA-P-TA and TA@Mg^{2+}. C. Synthetic route of GelMA.

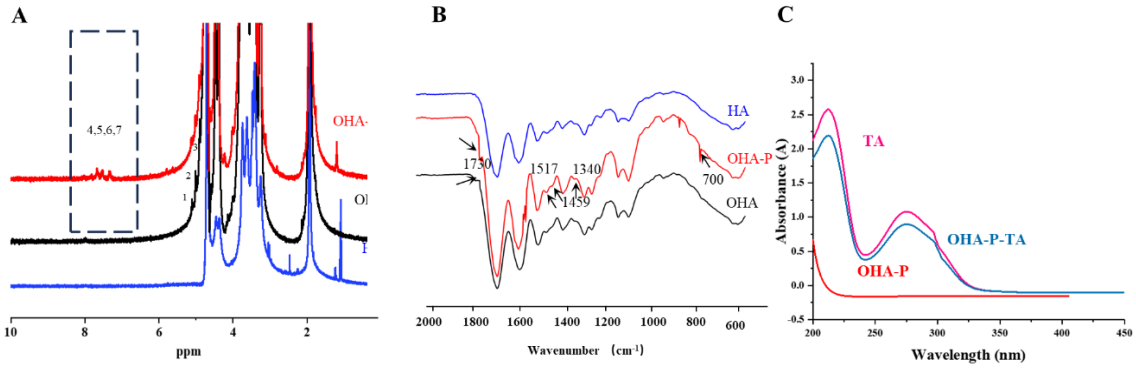

Fig. S2. Characterization analysis. A. ^{1}H NMR (D_2O) spectra of HA, OHA and OHA-P. B. The FTIR of HA, OHA and OHA-P. C. UV–vis absorption spectra of the aqueous solution of TA, OHA-P and OHA-P-TA.

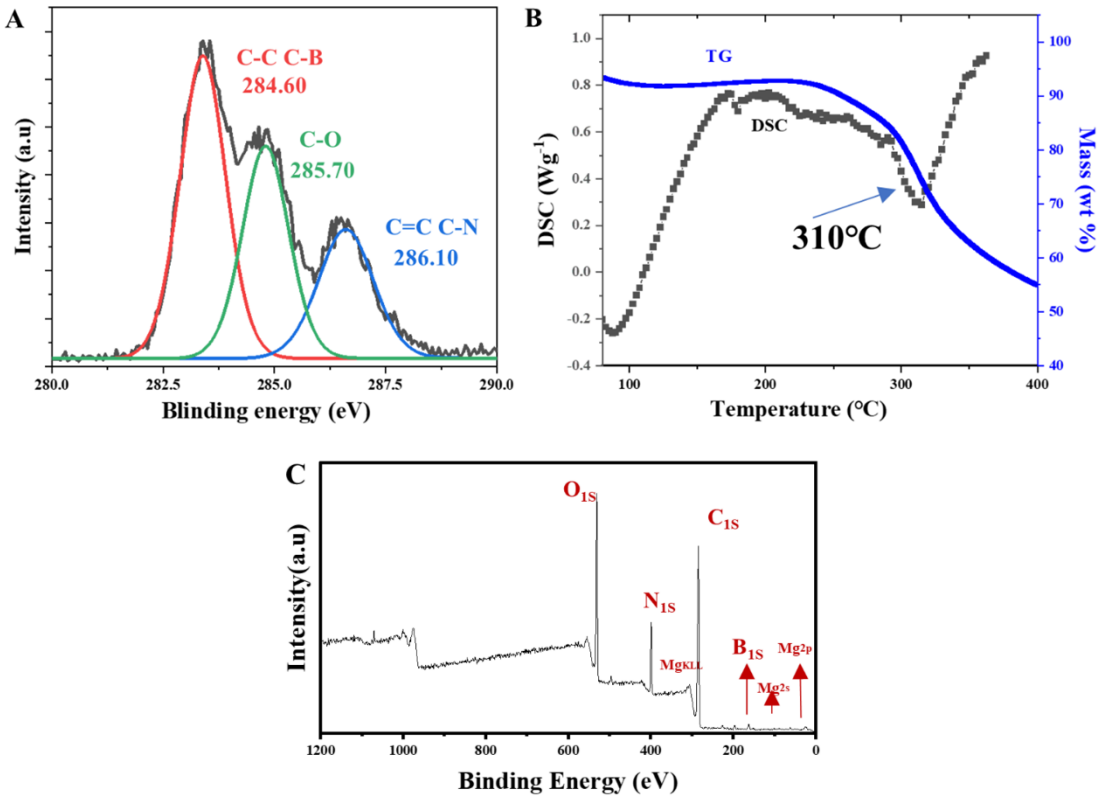

Fig. S3. Characterization analysis of OHA-P-TA/G/Mg^{2+}. A. High-resolution XPS spectra of C1s scan results of OHA-P-TA/G/Mg^{2+}. B. TG and DSC results of OHA-P-TA/G/Mg^{2+}. C. XPS characterization of OHA-P-TA/G/Mg^{2+} hydrogel.

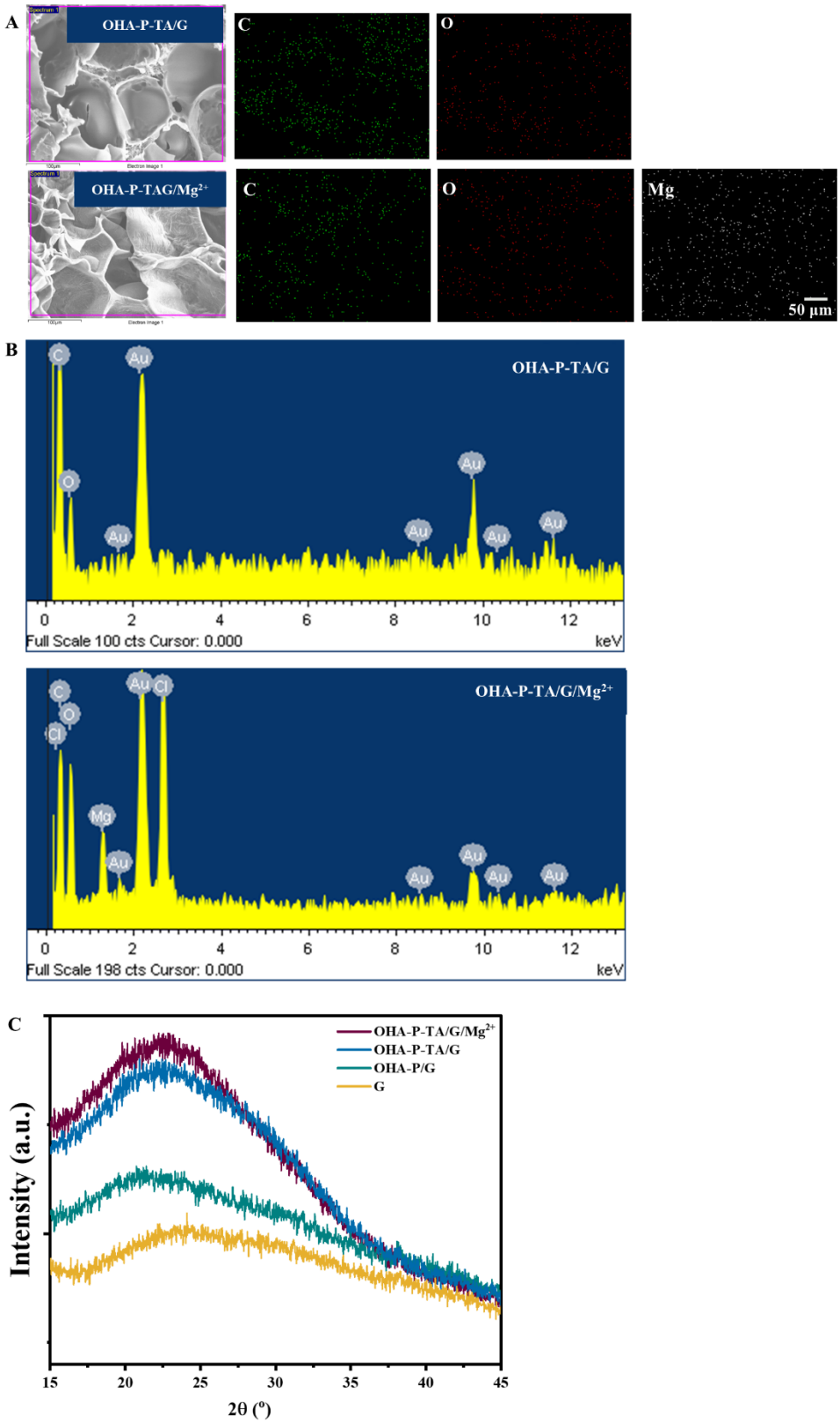

Fig. S4. EDS analysis and XRD spectra. A. Energy-dispersive spectrometry maps of the OHA-P-TA/G and OHA-P-TA/G/Mg^{2+} hydrogels; green, red, and white correspond to elemental C, O and Mg respectively. B. Element spectrum. C. XRD spectra of the G, OHA-P/G, OHA-P-TA/G and OHA-P-TA/G/Mg^{2+} hydrogels.

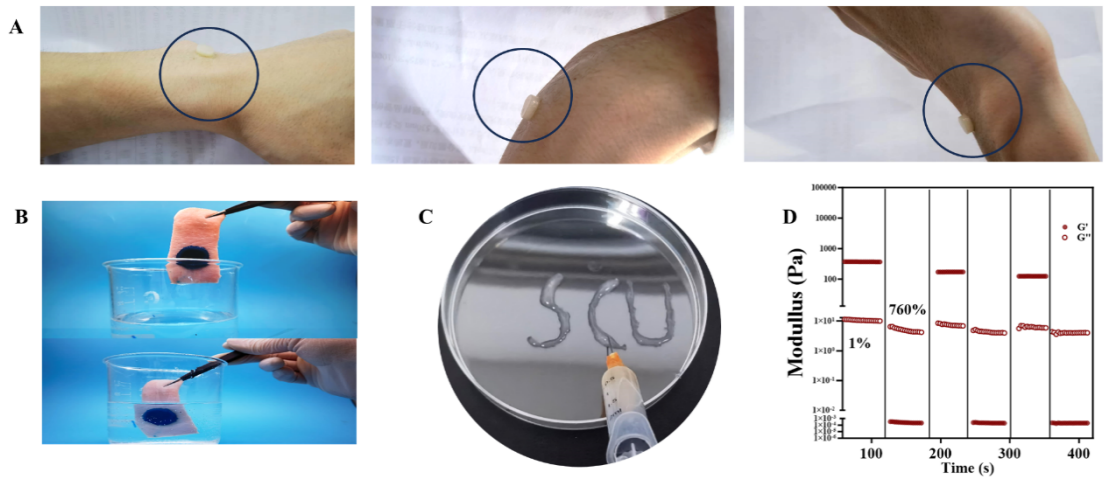

Fig. S5. Characterization analysis of adhesive capacity, injectable property and Self-healing ability. A. Representation of hydrogels applied on the human wrist, at varying angles. B. Images of hydrogels applied on skin tissue (from swine) with a shake in PBS. C. The injectable ability of Hydrogels. D. The storage modulus (G′) and loss modulus(G″) of OHA-P-TA/G/Mg^{2+} hydrogel when strain changes in alternating steps between 1% and 760%.

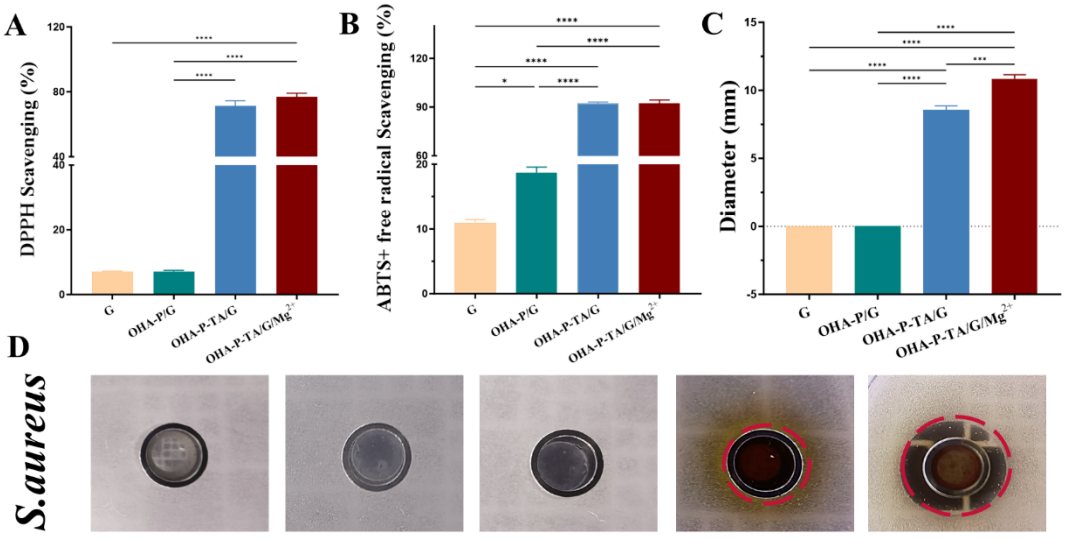

Fig. S6. Antioxidant and bactericidal ability of hydrogels. A. DPPH scavenging rate by different components of the hydrogels. B. ABTS+ free radical scavenging rate by different components of the hydrogels. C-D. The diameter of the inhibition ring of various hydrogels. Data are shown as mean ± SD, n = 3. *$p < 0.05$, **$p < 0.01$, ***$p < 0.001$, ****$p < 0.0001$.

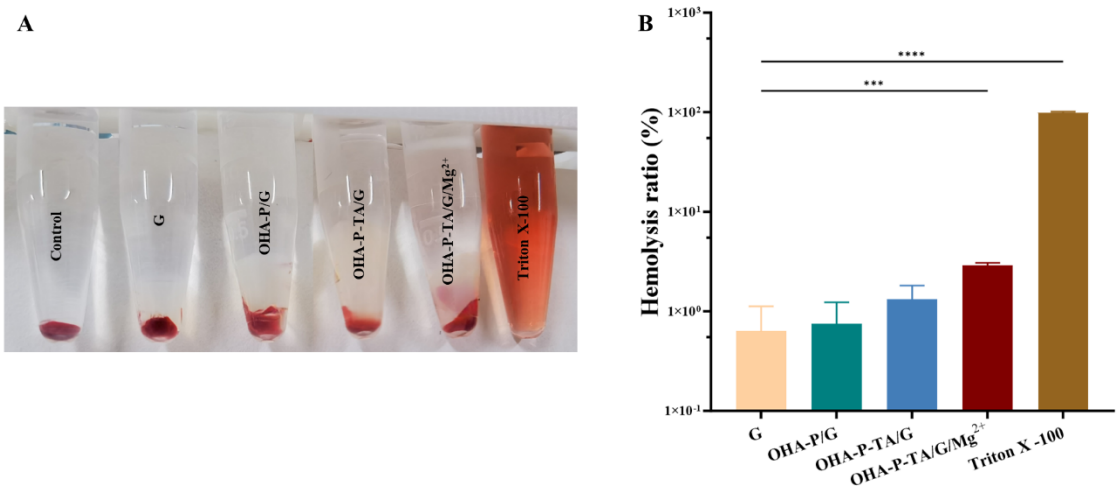

Fig. S7. Biocompatibility of hydrogels. A. Hemolytic photograph of PBS, different hydrogels, and Triton. B. Statistical hemolysis ratio. Data are shown as mean ± SD, n = 3. *$p < 0.05$, **$p < 0.01$, ***$p < 0.001$, ****$p < 0.0001$.

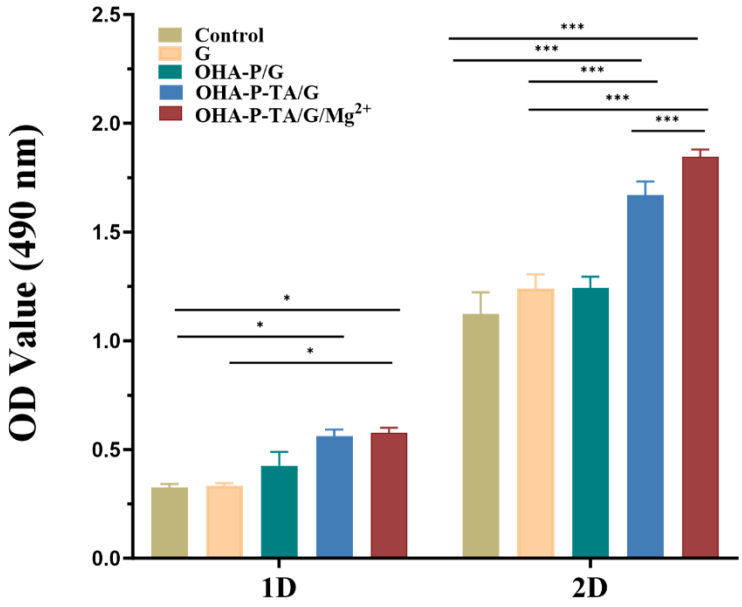

Fig. S8. Cell viability of RAW 264.7 cells after incubated with the different components of the hydrogels on day 1 and day 2. Data are shown as mean ± SD, n = 3. *$p < 0.05$, **$p < 0.01$, ***$p < 0.001$, ****$p < 0.0001$.

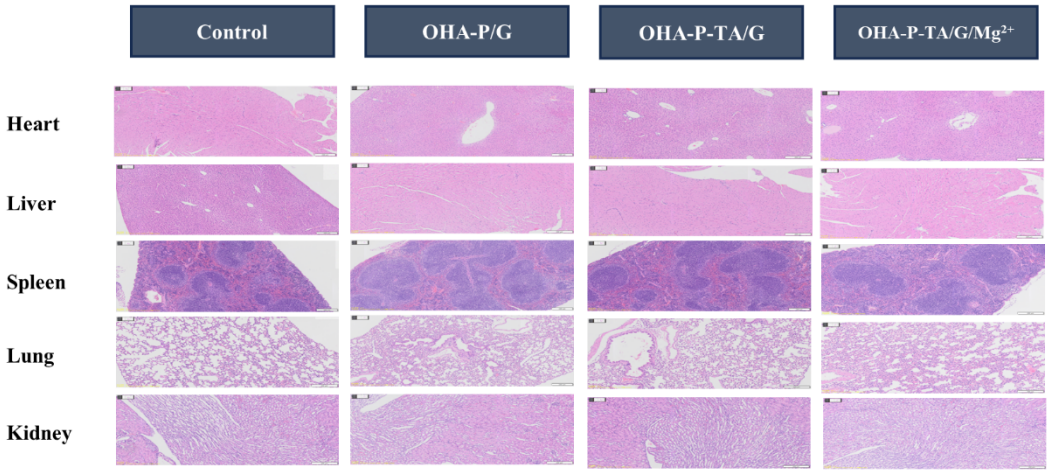

Fig. S9. H&E staining of heart, liver, spleen, lung, and kidney treated with the different the hydrogels on day 12 (scale bar: 200 μm).

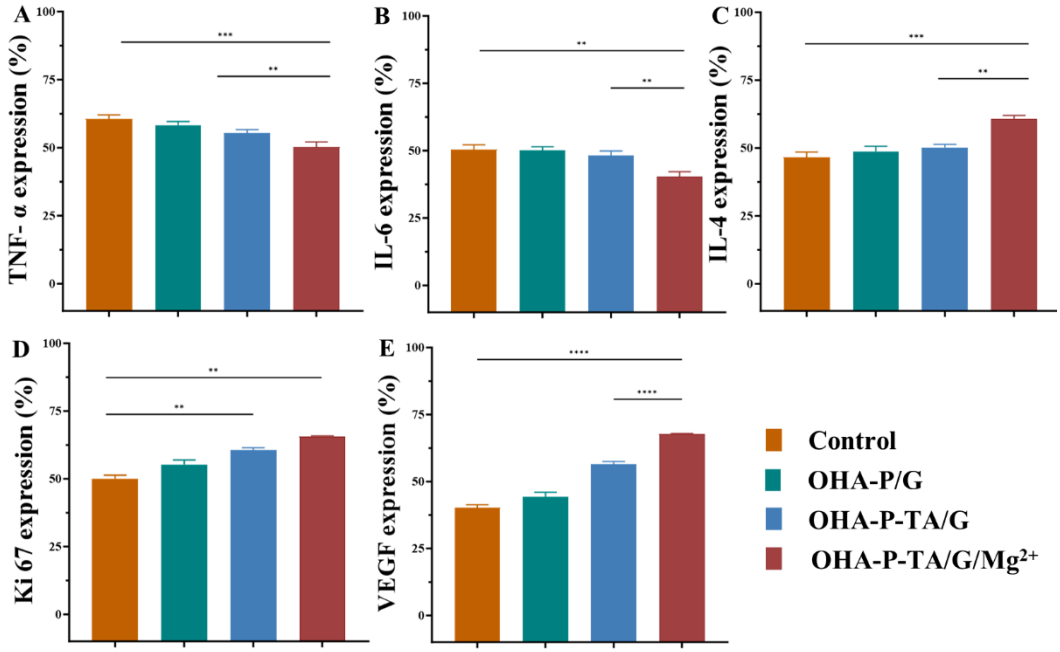

Fig. S10. Semi-quantitative analysis of immunohistochemical staining. A-E. The semi-quantitative expression of TNF-α, IL-6, IL-4, Ki67 and VEGF of the reformed epidermis in different groups on day 12. Data are shown as mean ± SD, n = 3. *p < 0.05, **p < 0.01, ***p < 0.001, ****p < 0.0001.

Table S1. Primers used to amplify mRNAs encoding

Primer	Sequence (5′-3′)
GAPDH-F	GGTGAAGGTCGGTGTGAACG
GAPDH-R	CTCGCTCCTGGAAGATGGTG
NF-KB-F	CCGGGAGCCTCTAGTGTAAT
NF-KB-R	TGCAAATCTGTTGCAAGGGG
TNF-α-F	CAACGGCTTGTATGCTGGAC
TNF-α-R	ACACCCTGGCAAGAGTTGTG
IL-6-F	GACAAAGCCAGAGTCCTTCAGA
IL-6-R	TGTGACTCCAGCTTATCTCTTGG
IL-4-F	AAGGACTTCATCGGCCTTGG
IL-4-R	CTTTGGTGTTGACTGCCACG
MagT-F	TCGGACCGTGCTGGAAGAAA
MagT -R	GCTGCTCCCGTGGATGTAAT
STAT3-F	TACACCAAGCAGCAGCTGAA
STAT3-R	CACTACCTGGGTCGGCTTC

Reference

1. K. H. Adolfsson, P. Huang, M. Golda-Cepa, H. Xu, A. Kotarba and M. Hakkarainen, Scavenging of DPPH by Persistent Free Radicals in Carbonized Particles, *Advanced Sustainable Systems*, 2023, **7**.
2. F. Li, X. Gou, D. Xu, D. Han, K. Hou, W. Fang and Y. Li, Improvement of tube formation model of cell: Application for acute hypoxia in in vitro study of angiogenesis, *Microvascular Research*, 2022, **140**, 104297.